Pediatr Radiol
DOI 10.1007/s00247-017-3918-6

ORIGINAL ARTICLE

Relationship between heart rate and quiescent interval of the cardiac cycle in children using MRI

Wei Zhang[1] · **Saivivek Bogale**[2] · **Farahnaz Golriz**[3] · **Rajesh Krishnamurthy**[4]

Received: 30 January 2017 / Revised: 8 May 2017 / Accepted: 2 June 2017

Abstract
Background Imaging the heart in children comes with the challenge of constant cardiac motion. A prospective electrocardiography-triggered CT scan allows for scanning during a predetermined phase of the cardiac cycle with least motion. This technique requires knowing the optimal quiescent intervals of cardiac cycles in a pediatric population.
Objective To evaluate high-temporal-resolution cine MRI of the heart in children to determine the relationship of heart rate to the optimal quiescent interval within the cardiac cycle.
Materials and methods We included a total of 225 consecutive patients ages 0–18 years who had high-temporal-resolution cine steady-state free-precession sequence performed as part of a magnetic resonance imaging (MRI) or magnetic resonance angiography study of the heart. We determined the location and duration of the quiescent interval in systole and diastole for heart rates ranging 40–178 beats per minute (bpm). We performed the Wilcoxon signed rank test to compare the duration of quiescent interval in systole and diastole for each heart rate group.
Results The duration of the quiescent interval at heart rates <80 bpm and >90 bpm was significantly longer in diastole and systole, respectively ($P<.0001$ for all ranges, except for 90–99 bpm [$P=.02$]). For heart rates 80–89 bpm, diastolic interval was longer than systolic interval, but the difference was not statistically significant ($P=.06$). We created a chart depicting optimal quiescent intervals across a range of heart rates that could be applied for prospective electrocardiography-triggered CT imaging of the heart.
Conclusion The optimal quiescent interval at heart rates <80 bpm is in diastole and at heart rates ≥90 bpm is in systole. The period of quiescence at heart rates 80–89 bpm is uniformly short in systole and diastole.

Keywords Computed tomography · Children · Electrocardiography · Heart · Magnetic resonance imaging · Quiescent interval

Introduction

Multi-detector CT imaging continues to evolve as a powerful diagnostic tool for the noninvasive imaging of cardiac and coronary pathology [1]. Imaging of the heart in children has specific challenges related to constant cardiac motion and the short quiescent phase of the cardiac cycle in the setting of high heart rates, making it difficult to image the heart without substantial motion artifact. Electrocardiography (ECG)-triggered CT scans minimize motion artifact by reconstructing images during the optimal motion-free period of the cardiac cycle. Identification of the quiescent phase is typically performed with a retrospective ECG-gating scan, which allows for reconstruction of images across the entire cardiac cycle. This approach provides a reliable means of identifying the phase with the least cardiac motion, but it involves approximately 1.5–3

✉ Wei Zhang
wxzhang1@texaschildrens.org

[1] E. B. Singleton Department of Pediatric Radiology
Texas Children's Hospital,
6701 Fannin St., Houston, TX 77030, USA

[2] Department of Radiology, Baylor University Medical Center,
Dallas, TX, USA

[3] Department of Radiology, Baylor College of Medicine,
Houston, TX, USA

[4] Department of Diagnostic Radiology
Nationwide Children's Hospital,
Columbus, OH, USA

Published online: 25 July 2017

times the radiation dose of an ungated CT [2–4]. With the advent of prospective ECG-triggered CT scans, there is a potential to reduce patient radiation exposure by scanning only during a predetermined phase of the cardiac cycle. This technique requires prediction of the optimal phase of the cardiac cycle for image acquisition. MRI of the heart offers higher temporal resolution than cardiac CT scans because of MRI's utility in imaging the heart over several cardiac cycles. Because of its increased temporal resolution, cardiac MRI imaging data can be used to construct a database of the optimal motion-free intervals for cardiac imaging in relation to heart rate.

In this study, we retrospectively reviewed high-temporal-resolution cine MRIs of the heart to determine the relationship of heart rate to the optimal quiescent interval within the cardiac cycle, and to derive a chart depicting optimal intervals for cardiac imaging across a range of heart rates.

Materials and methods

Our institutional review board approved this retrospective study and waived the requirement for informed consent.

Patient population

We included 225 children who had clinically indicated MRI/MR angiography of the heart from June 2006 to May 2011. Children who had high-temporal-resolution cine steady-state free-precession (SSFP) sequence performed as part of the MR coronary angiography protocol were selected for a chart review. The indications for the MRI study included: 26 (12%) screen for arrhythmogenic right ventricular cardiomyopathy, 44 (20%) coronary diseases, 19 (8%) repaired tetralogy of Fallot, 32 (14%) cardiomyopathy, 39 (17%) aortic diseases, 21 (9%) post palliation of single ventricle and 44 (20%) other two-ventricular repair such as transposition of the great arteries or truncus arteriosus.

Overall the mean age was 8.4±6.3 years (range 0–18 years) and mean heart rate was 91.3±25.6 bpm (range 40–178 bpm). Grouped demographic data are displayed in Table 1.

Imaging protocol

All MRIs were performed on Philips Achieva 1.5-T scanners (Philips Healthcare, Best, the Netherlands). The high-temporal-resolution SSFP sequence was performed in a four-chamber view, with the child breathing freely, with the following parameters: repetition time 2.8 ms, echo time 1.4 ms, flip angle 30°, echo train length 11, slice thickness 4–8 mm, field of view (FOV) 20–40 cm based on patient size, matrix 192×116, spatial resolution ranging from 1.7×2.1 mm to 2.1×2.5 mm and shot duration 20–30 ms (adjusted to obtain 50 phases across the cardiac cycle). The temporal resolution ranged 8–28 ms (mean temporal resolution 14.5 ms).

Image analysis

The cine MR datasets were reviewed by a radiologist (R.K.) with 12 years of post-fellowship experience in pediatric cardiac imaging. The right atrioventricular groove was the primary target for assessing motion, although the assessment of the quiescent interval was corroborated using the free wall of the right and left ventricles. The location of the quiescent interval in systole and diastole in terms of the percentage of the RR interval, as well as the duration of the quiescent interval in milliseconds, were calculated using the following method:

- The image numbers that marked the beginning and end of the quiescent interval in systole and diastole were identified.
- The number of static images within the systolic and diastolic quiescent intervals was identified by calculating the difference between the beginning and the end image numbers.
- The quiescent interval percentage (quiescent duration as a percentage of each heartbeat) was the number of static images divided by 50, the total number of images obtained across one heartbeat.
- The quiescent interval location in terms of percentage of the cardiac cycle was the beginning and end image number of the quiescent interval divided by 50.
- Based on the mean heart rate of a patient, the RR interval was calculated in milliseconds.
- The duration of quiescent interval in milliseconds was the RR interval × the quiescent interval percentage.

Data collection

For each subject, we collected the following information: age, heart rate (minimum, maximum and mean heart rates during SSFP sequence acquisition), duration of systole and diastole, location of the quiescent interval in systole and diastole as a function of the percentage of the cardiac cycle, and duration of quiescent interval in systole and diastole. Heart rate variability for each child was calculated as the difference between maximum and minimum heart rates.

Statistical analysis

Mean heart rates were grouped in ranges of 10 (<60, 60–69, 70–79, 80–89,90–99, 100–109, 110–119, 120–129, ≥130 bpm). We

Table 1 Grouped demographic data of patients

Heart rate range (bpm)	Number of patients	Age (years)	Mean heart rate (bpm)	Heart rate variability (bpm)
<60	25	15.7 ± 2.9	53.4 ± 4.3	6.9 ± 5.2
60–69	24	14.1 ± 3.6	64.6 ± 3.2	11.2 ± 6.7
70–79	25	12.7 ± 4.2	74.3 ± 3.3	11.7 ± 4.5
80–89	44	9.8 ± 4.3	83.9 ± 3.1	12.2 ± 1.4
90–99	26	7.2 ± 4.9	94.9 ± 2.7	16.2 ± 4.9
100–109	24	3.7 ± 4.1	103.8 ± 2.8	18.2 ± 1.0
110–119	23	4.6 ± 5.2	113.1 ± 2.6	22.6 ± 4.2
120–129	16	1.0 ± 1.3	125.2 ± 3.0	26.8 ± 1.5
>130	18	0.7 ± 0.9	142.0 ± 13.0	34.5 ± 6.8

bpm beats per minute

used the Wilcoxon signed rank test to compare the static durations of systolic and diastolic phases for each heart rate group. Two-tailed *P*-values <0.05 were considered statistically significant. Using these data, we created a chart matching heart rate range to the optimal quiescent cardiac phase.

Results

Mean duration of the quiescent interval in systole and diastole

The mean duration of quiescent interval in diastole had a large variation with respect to the heart rate. It decreased from 335 ms to 38 ms when the heart rate increased from <60 bpm to ≥130 bpm. On the other hand, the mean duration of the quiescent interval in systole was relatively stable with respect to the heart rate. It varied between 72 ms and 106 ms for different heart rates.

The comparisons between durations of systolic and diastolic quiescent intervals by heart rate range are described in Table 2 and Fig. 1. The quiescent durations of systole and diastole were significantly different at all heart rate ranges except for 80–89 bpm. For heart rate ranges lower than 80 bpm, the quiescent interval was longer in diastole. When the range was higher than 90 bpm, the systolic quiescent interval was significantly longer. The *P*-values were all <0.0001 except for the range 90–99 bpm, where the *P*-value was 0.03. For heart rates at 80–89 bpm, diastolic interval was on average longer than systolic interval; however the difference was not statistically significant (*P* = .08).

Optimal quiescent interval

The optimal quiescent interval for image acquisition was chosen to be in either diastole or systole based on which one had a longer duration. The center of the optimal quiescent interval for a given heart rate was calculated in terms of percentage of the RR interval for each heart rate group (Table 3 and Fig. 2). The optimal interval center shifted from 72.9% to 85.4% when heart rate increased from 60 bpm to 89 bpm and a diastolic interval was chosen. With higher heart rates, the optimal interval center stayed in a range between 50.8% and 55.1%, and a systolic interval was chosen.

Table 2 Comparison of mean duration of motionless phase in systole and diastole

Heart rate range (bpm)	Systolic static duration (ms)	Diastolic static duration (ms)	*P*-value	Optimal phase
<60	80 ± 20 (44–126)	335 ± 99 (92–485)	<0.0001	Diastole
60–69	72 ± 23 (39–124)	212 ± 83 (70–340)	<0.0001	Diastole
70–79	77 ± 38 (30–186)	131 ± 40 (63–203)	<0.0001	Diastole
80–89	87 ± 38 (27–195)	96 ± 37 (54–223)	0.08*	Diastole*
90–99	87 ± 28 (40–148)	71 ± 34 (36–155)	0.03	Systole
100–109	105 ± 33 (47–202)	61 ± 21 (24–119)	<0.0001	Systole
110–119	106 ± 38 (32–171)	49 ± 20 (21–84)	<0.0001	Systole
120–129	105 ± 35 (56–184)	38 ± 14 (10–57)	<0.0001	Systole
>130	97 ± 22 (46–135)	38 ± 15 (16–72)	<0.0001	Systole

bpm beats per minute

*Diastolic static durations were not statistically significantly different from systolic durations in this group

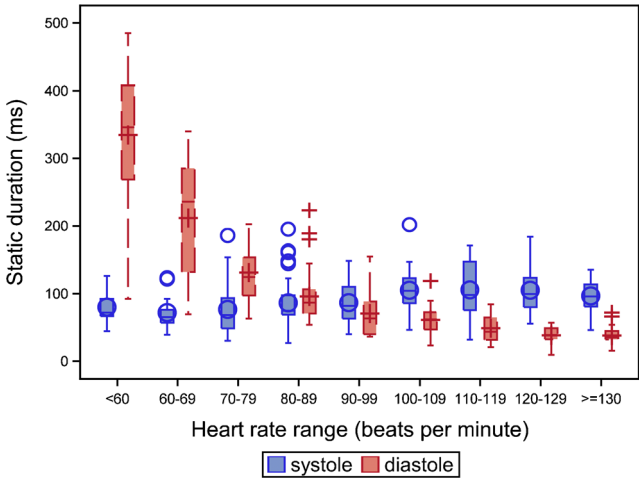

Fig. 1 Boxplot of mean duration of motionless phase in systole and diastole by heart rate range. Bars indicate 5% and 95% quantiles. Boxes indicate 25%, 50% and 75% quantiles. Blue circles between bars represent mean values, outside of bars are outliers of the systolic phase. Red plus signs between bars represent mean values, outside of bars are outliers of the diastolic phase

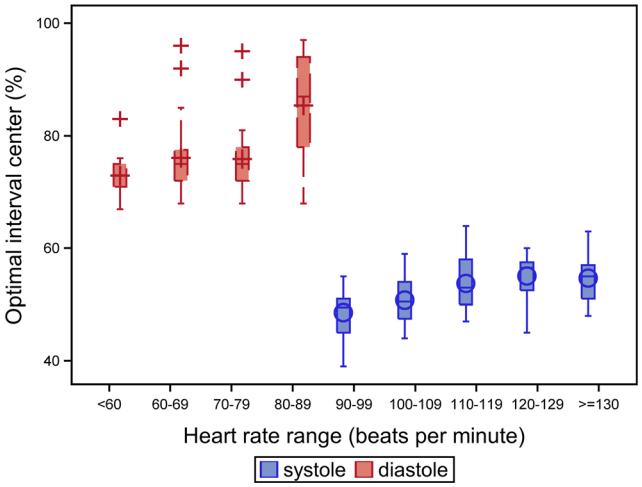

Fig. 2 Boxplot of center of optimal quiescent interval as a percentage of the cardiac cycle by heart Rate Range. Bars indicate 5% and 95% quantiles. Boxes indicate 25%, 50% and 75% quantiles. Blue circles between bars represent mean values of the systolic phase. Red plus signs between bars represent mean values, outside of bars are outliers of the diastolic phase

Discussion

The application of radiation dose saving techniques based on prospective ECG-triggering requires selection of the optimal cardiac phase before scanning. In our study, we determined the location of quiescent cardiac intervals across a range of heart rates with temporal resolution of 8–28 ms. Based on these data we recommend that scanning in prospective ECG-triggered cardiac CT should be performed in diastole for children with heart rates <80 bpm and in systole for those with heart rates ≥90 bpm. In patients with heart rates at 80–89 bpm, the period of quiescence is uniformly short in systole and diastole.

Previous studies with retrospective ECG-gating multi-detector CT have shown that diastolic reconstructions provide superior image quality compared with systolic reconstructions in patients with heart rates <60 bpm [5–15]. However the literature is controversial for higher heart rates. For example, Leschka et al. [7], in a study using 64-multi-detector CT, found that for heart rates up to 88 bpm the best cardiac phase for image reconstruction was in diastole (60–65% of RR interval). In a more recent study involving 64-detector dual-source CT, Leschka et al. [9] concluded that dual-source CT coronary angiography provides the best image quality for various heart rates (35–117 bpm) at diastole (70% of RR interval). In contrast with these observations, several investigations have demonstrated that as diastolic diastasis shortens in patients with high heart rates, optimal reconstruction time shifts to late systole (isovolumetric relaxation of the ventricles) [5, 6, 8, 10–14]. Leschka et al. [8], using a 64-detector CT scanner, suggested a transition from the diastolic phase (50–80% of RR interval) for heart rates <85 bpm to the systolic phase (25–40% of RR interval) in heart rates ≥85 bpm (85–102 bpm) for

Table 3 Center of optimal quiescent interval as a percentage of the cardiac cycle

Heart rate range (bpm)	Systolic quiescent interval center %	Diastolic quiescent interval center %	Optimal interval center %
<60	34.3 ± 2.8	72.9 ± 3.2	72.9 ± 3.2
60–69	38.5 ± 4.2	76.1 ± 6.7	76.1 ± 6.7
70–79	42.4 ± 3.8	76.6 ± 6.0	76.6 ± 6.0
80–89	45.4 ± 4.3	85.4 ± 8.8	85.4 ± 8.8*
90–99	48.6 ± 4.0	90.2 ± 8.5	48.6 ± 4.0
100–109	50.8 ± 4.1	93.5 ± 4.1	50.8 ± 4.1
110–119	53.7 ± 4.5	94.9 ± 2.1	53.7 ± 4.5
120–129	55.1 ± 3.9	94.1 ± 4.6	55.1 ± 3.9
>130	54.7 ± 4.4	94.7 ± 3.0	54.7 ± 4.4

bpm beats per minute

*Diastolic static durations were not statistically significantly different from systolic durations in this group

optimal image reconstruction. Similarly, Seifarth et al. [11] compared systolic and diastolic reconstruction intervals using 64-detector dual-source CT and demonstrated that in patients with heart rates >80 bpm (80–119 bpm), systolic reconstruction often offers superior image quality. Araoz et al. [13] found the optimal image quality at 35–45% of RR interval for heart rates >70 bpm using 64-detector dual-source CT. Weustink et al. [12] reported that with heart rates at ≥80 bpm (80–112 bpm) fewer motion artifacts occur in systole (31–47% of RR interval) and in patients with heart rates at 66–79 bpm the use of both systolic and diastolic data sets permits high-quality imaging of coronary arteries. Goetti et al. [14] demonstrated that scanning at 30% of RR interval during high-pitch helical mode on 128-detector dual-source CT in patients with heart rates ≥70 bpm significantly improved the sharpness of coronary arteries [14]. Although these studies support systolic reconstruction in patients with high heart rates, the threshold heart rate to shift from diastolic reconstruction to systolic reconstruction and the optimal location for the center of acquisition window at different heart rates is still unclear.

In this study, we found a significant decrease in the quiescent period of the heart as well as an increase in heart rate variability at higher rates. These findings explain why current protocols of prospective ECG-triggered CT angiography even on modern scanners might not eliminate the motion artifact from cardiac pulsation in children with high heart rates — the data acquisition window might exceed the quiescent period of the heart. The most recent advances in CT technology are wide-detector scanner (320-detector) and dual-source CT. Acquisition of temporally uniform data with a wide-detector scanner allows for retrospective half-scan reconstruction of the optimal motionless cardiac phase across the entire spectrum of the cardiac cycle spanned by the rotation time, which overcomes the limitations caused by heart rate variability [16]. However even the second-generation 320-detector scanner has a temporal resolution of 137 ms, which exceeds the quiescent period of the heart at heart rates >80 bpm. The 128-detector dual-source CT has the high temporal resolution of 66 ms, which often falls within the quiescent period of the heart, even in children with a high heart rate. However, because the entire volume of interest is acquired continuously within one cardiac cycle in high-pitch helical mode, the whole data acquisition time (approximately 200–300 ms) exceeds the quiescent period of the heart in people with a heart rate faster than 60 bpm [17], resulting in temporally non-uniform images. Using step-and-shoot mode in dual-source CT allows for the use of ECG padding for children with high heart rate variability. However this mode is still not ideal for evaluation of coronary arteries and intracardiac structures because of stair-step artifacts, temporally non-uniform images, and longer scan times (approximately 2 s), in addition to the higher radiation dose associated with this technique [3, 18]. The optimal solution is temporally uniform volumetric data acquisition with high temporal resolution (<75 ms), a technique that is unavailable in commercial CT scanners.

Our study has some limitations. First, we evaluated the motion of the right atrioventricular groove in two dimensions but did not examine through-plane motion. However Johnson et al. [19] measured the 3-D motion of the coronary arteries with MRI and noted that the quiescent period of coronary arteries across anterior–posterior, right–left and cranial–caudal directions are similar. Another important limitation is that our data were obtained from a group of children with congenital heart disease, which could change the motion pattern of the right atrioventricular groove when compared to normal patients. The quiescent interval might vary with the type of disease as well. The high temporal resolution SSFP images were obtained over several beats, and the standard deviation of the RR interval of the beats was not recorded as a check of heart rate variability because of the retrospective nature of the study. Although our study is distinct regarding the use of high-temporal-resolution MRI data, this technique had a low spatial resolution when compared to some previous studies using multi-detector CT. However no cross-sectional imaging modality at present provides adequately high temporal and spatial resolution to permit assessment of the coronary arteries throughout the cardiac cycle. Finally, no data were acquired using CT. Therefore the translation of the obtained quiescent intervals to cardiac CT imaging is theoretical.

Conclusion

Our study determined the location and duration of the quiescent phase of the heart across a wide range of heart rates. These data could be applied to prospectively select the optimal cardiac phase for ECG-triggered CT angiography. Further refinements in CT scanner technology, which allow prospective ECG-triggered volumetric coverage of the whole heart in single acquisition with improved temporal resolution, might permit evaluation of the heart and coronary arteries with low radiation dose and minimal motion artifacts.

Compliance with ethical standards

Conflicts of interest None

References

1. Lee T, Tsai IC, Fu YC et al (2006) Using multidetector-row CT in neonates with complex congenital heart disease to replace diagnostic cardiac catheterization for anatomical investigation: initial experiences in technical and clinical feasibility. Pediatr Radiol 36:1273–1282
2. Jin KN, Park EA, Shin CI et al (2010) Retrospective versus prospective ECG-gated dual-source CT in pediatric patients with

congenital heart diseases: comparison of image quality and radiation dose. Int J Cardiovasc Imaging 26:63–73
3. Paul JF, Rohnean A, Sigal-Cinqualbre A (2010) Multidetector CT for congenital heart patients: what a paediatric radiologist should know. Pediatr Radiol 40:869–875
4. Ben Saad M, Rohnean A, Sigal-Cinqualbre A et al (2009) Evaluation of image quality and radiation dose of thoracic and coronary dual-source CT in 110 infants with congenital heart disease. Pediatr Radiol 39:668–676
5. Herzog C, Arning-Erb M, Zangos S et al (2006) Multi-detector row CT coronary angiography: influence of reconstruction technique and heart rate on image quality. Radiology 238:75–86
6. Wintersperger BJ, Nikolaou K, von Ziegler F et al (2006) Image quality, motion artifacts, and reconstruction timing of 64-slice coronary computed tomography angiography with 0.33-second rotation speed. Investig Radiol 41:436–442
7. Leschka S, Husmann L, Desbiolles LM et al (2006) Optimal image reconstruction intervals for non-invasive coronary angiography with 64-slice CT. Eur Radiol 16:1964–1972
8. Leschka S, Wildermuth S, Boehm T et al (2006) Noninvasive coronary angiography with 64-section CT: effect of average heart rate and heart rate variability on image quality. Radiology 241:378–385
9. Leschka S, Scheffel H, Desbiolles L et al (2007) Image quality and reconstruction intervals of dual-source CT coronary angiography: recommendations for ECG-pulsing windowing. Investig Radiol 42: 543–549
10. Husmann L, Leschka S, Desbiolles L et al (2007) Coronary artery motion and cardiac phases: dependency on heart rate — implications for CT image reconstruction. Radiology 245:567–576
11. Seifarth H, Wienbeck S, Pusken M et al (2007) Optimal systolic and diastolic reconstruction windows for coronary CT angiography using dual-source CT. AJR Am J Roentgenol 189:1317–1323
12. Weustink AC, Mollet NR, Pugliese F et al (2008) Optimal electrocardiographic pulsing windows and heart rate: effect on image quality and radiation exposure at dual-source coronary CT angiography. Radiology 248:792–798
13. Araoz PA, Kirsch J, Primak AN et al (2009) Optimal image reconstruction phase at low and high heart rates in dual-source CT coronary angiography. Int J Cardiovasc Imaging 25:837–845
14. Goetti R, Feuchtner G, Stolzmann P et al (2010) High-pitch dual-source CT coronary angiography: systolic data acquisition at high heart rates. Eur Radiol 20:2565–2571
15. Horii Y, Yoshimura N, Hori Y et al (2011) Relationship between heart rate and optimal reconstruction phase in dual-source CT coronary angiography. Acad Radiol 18:726–730
16. Jadhav SP, Golriz F, Atweh LA et al (2015) CT angiography of neonates and infants: comparison of radiation dose and image quality of target mode prospectively ECG-gated 320-MDCT and ungated helical 64-MDCT. AJR Am J Roentgenol 204:W184–W191
17. Nie P, Wang X, Cheng Z et al (2012) Accuracy, image quality and radiation dose comparison of high-pitch spiral and sequential acquisition on 128-slice dual-source CT angiography in children with congenital heart disease. Eur Radiol 22:2057–2066
18. Paul JF, Rohnean A, Elfassy E, Sigal-Cinqualbre A (2011) Radiation dose for thoracic and coronary step-and-shoot CT using a 128-slice dual-source machine in infants and small children with congenital heart disease. Pediatr Radiol 41:244–249
19. Johnson KR, Patel SJ, Whigham A et al (2004) Three-dimensional, time-resolved motion of the coronary arteries. J Cardiovasc Magn Reson 6:663–673